water

MDPI

Article

Comparative Study on Sediment Delivery from Two Small Catchments within the Lena River, Siberia

Kirill Maltsev * and Maxim Ivanov

Department of Landscape Ecology, Institute of Ecology and Environment, Kazan Federal University, Kazan 4200097, Russia

* Correspondence: mlcvkirill@mail.ru

Abstract: This paper studies the possibility of using the WaTEM/SEDEM model to assess sediment yield from the catchment area within the Lena River catchment. The study was carried out based on a comparison of predicted data and measured data of the suspended sediment yield at the gauging stations of the state monitoring network of Russia. The study was performed within two areas, with plain and mountainous relief. The first site is located within the catchment area of the river Chara with an area of 4150 km^2. The second site rests on the catchment area of the Lena River between the Tabaginskiy and Kangalassky capes near Yakutsk city. The catchment area of this site is 15,740 km^2. The values of sediment yield from the "Yakutsk" catchment area are in much better agreement with the values of the measured sediment yield values than in the "Chara" catchment area. The predicted sediment yield from the study area remained almost unchanged from the period 1986–2019 and amounted to 3.5 t/km^2, while the suspended sediment yield in the Lena at the Tabaga gauging station slightly increased from 7 to 9.45 t/km^2 per year.

Keywords: sediment yield; soil erosion; WaTEM/SEDEM; Lena River

Citation: Maltsev, K.; Ivanov, M. Comparative Study on Sediment Delivery from Two Small Catchments within the Lena River, Siberia. *Water* **2022**, *14*, 3055. https://doi.org/10.3390/w14193055

Academic Editor: Sergey R. Chalov

Received: 25 August 2022
Accepted: 23 September 2022
Published: 28 September 2022

1. Introduction

The Lena River is the largest river in the Arctic, of which most of the catchment area is located in the zone of permafrost. Modern climate change and permafrost degradation have led to a change in the flow of water, sediment, and chemicals into the Arctic Ocean [1]. The dynamics of sediment yield from the Lena River catchment deserve special attention, as it affects many processes, such as the rate of siltation of reservoirs and the mass of incoming pollutants. At the same time, sediment yield from the catchment area is an indicator of the intensity of the erosion processes in the catchment area. It is necessary to apply both modeling methods and field instrumental assessment methods since each of them have its strengths and weaknesses when analyzing the sediment yield of each area. Wherein, it is impossible to estimate the contribution of the catchment component from a large area to the sediment yield of the river without the use of erosion models.

Currently, there are different classifications of erosion models that are used, among other things, to assess the suspended sediment yield. Most researchers distinguish conceptual, empirical, and physically based models [2].

The empirical models are based on observations of the environment that can be statistically quantified without a detailed description of the causes of a physical process [3]. Examples of empirical models are USLE [4], RUSLE [5], and MUSLE [6]. Physically based models are based on the physics of flow and sediment transport processes and their interaction with the transfer of mass, momentum, and energy [7]. Examples of physically based models are: WEPP [8]; LISEM [9]; EROSION 3D [10]; EUROSEM [11].

Conceptual models are a combination of empirical and physically based models [12], examples are: WaTEM/SEDEM [13,14]; RUSLE2 [15]; MMF [16]; SWAT [17,18].

The studied territory of the Lena River catchment has repeatedly become the object of study of erosion processes. Here we can mention works performed by: employees of

the Russian Academy of Sciences [19], Moscow State University [20], and Kazan Federal University [21]. In addition, soil erosion was assessed in the Lena River catchment as part of the larger project "An assessment of the global impact of 21st-century land use change on soil erosion" [22]. However, within the framework of all these studies, soil losses within river catchments were performed without taking into account the process of accumulation of part of the eroded material or without assessing the suspended sediment yield from the catchment area in the river. In addition to erosion losses, it is necessary to know how this material will accumulate along the path of sediment transport from slopes to the hydrographic network for a spatial assessment of the erosion-accumulation budget of sediments and a quantitative assessment of sediment yield. The processes of accumulations of material down the slope are largely determined by the sediment connectivity of the territory. Several indicators are now used to determine the sediment connectivity: sediment delivery ratio (SDR) [23–25]; index of connectivity (I.C.) [26–28]; travel time [29,30]; transport capacity [14,31].

One of the most commonly used approaches is the use of the transport capacity within the Water and Tillage Erosion Model and Sediment Delivery Model (WaTEM/SEDEM) model [2], due to the small amount of data needed for calculations and the high quality of results obtained. M. Sheng and H. Fang [32] have researched the progress in the WaTEM/SEDEM model and its application prospect in the studies on sediment transport. The WaTEM/SEDEM has been developed at the Physical and Regional Geography Research Group, KU Leuven University, Belgium. It is a spatially distributed soil erosion and sediment delivery model. Compared to other more sophisticated dynamic models, this model requires minimal data input and the model structure is simple. The WaTEM/SEDEM has data requirements almost similar to the RUSLE model and it can assess both water and tillage erosion; moreover, it can spatially model the soil erosion and sediment deposition rates, as well as the soil redistribution patterns. The WaTEM/SEDEM model has been used quite frequently around the world [2]. For example, WaTEM/SEDEM model studies were conducted in Spain in 68 river catchments [33], in Italy in 40 river catchments [34], Belgium in 24 river catchments [13], and in central and northern Mongolia [35].

The model is still rarely used within the territory of Russia. It can be noted in the traditional agricultural regions in the south of the European part of Russia, within the Belgorod region [31], and the east Russian Plain [36]. This model is rarely used in the predominantly non-agricultural territories of Siberia and the Lena River catchment.

Accordingly, the purpose of this work is to assess the possibility of using the WaTEM/SEDEM model within two local catchment areas in the Lena River catchment, with different topography to quantify the sediment yield from the catchment area, and its dynamics over the past few decades due to changes in land use and precipitation intensity.

2. Materials and Methods

2.1. Study Area

The study areas are located within the plain and mountainous relief. The first mountain site is located within the catchment area of the gauging station in the town of Chara (Figure 1) and has an area of 4150 km^2. The «Chara» site is located within the Stanovoi upland and has elevations ranging from 700 to 3060 m, with an average elevation of 1449 m (Table 1). The geological structure of the site is mainly represented by pre-Quaternary acid plutonic and metamorphic rocks in the highland part of the site, as well as unconsolidated sediments and mixed sedimentary rocks in the Chara River valley [37]. The second plain catchment area near the city of Yakutsk is located between the Tabaginskiy and Kangalassky capes and has an area of 15,740 km^2. The «Yakutsk» site is located within the Prilenskoye plateau and has elevations ranging from 74 to 423 m, with an average elevation of 223 m (Table 1). The geological structure of the site is mainly represented by siliciclastic sedimentary rocks in the elevated part of the site, as well as alluvium rocks closer to the Lena channel [37].

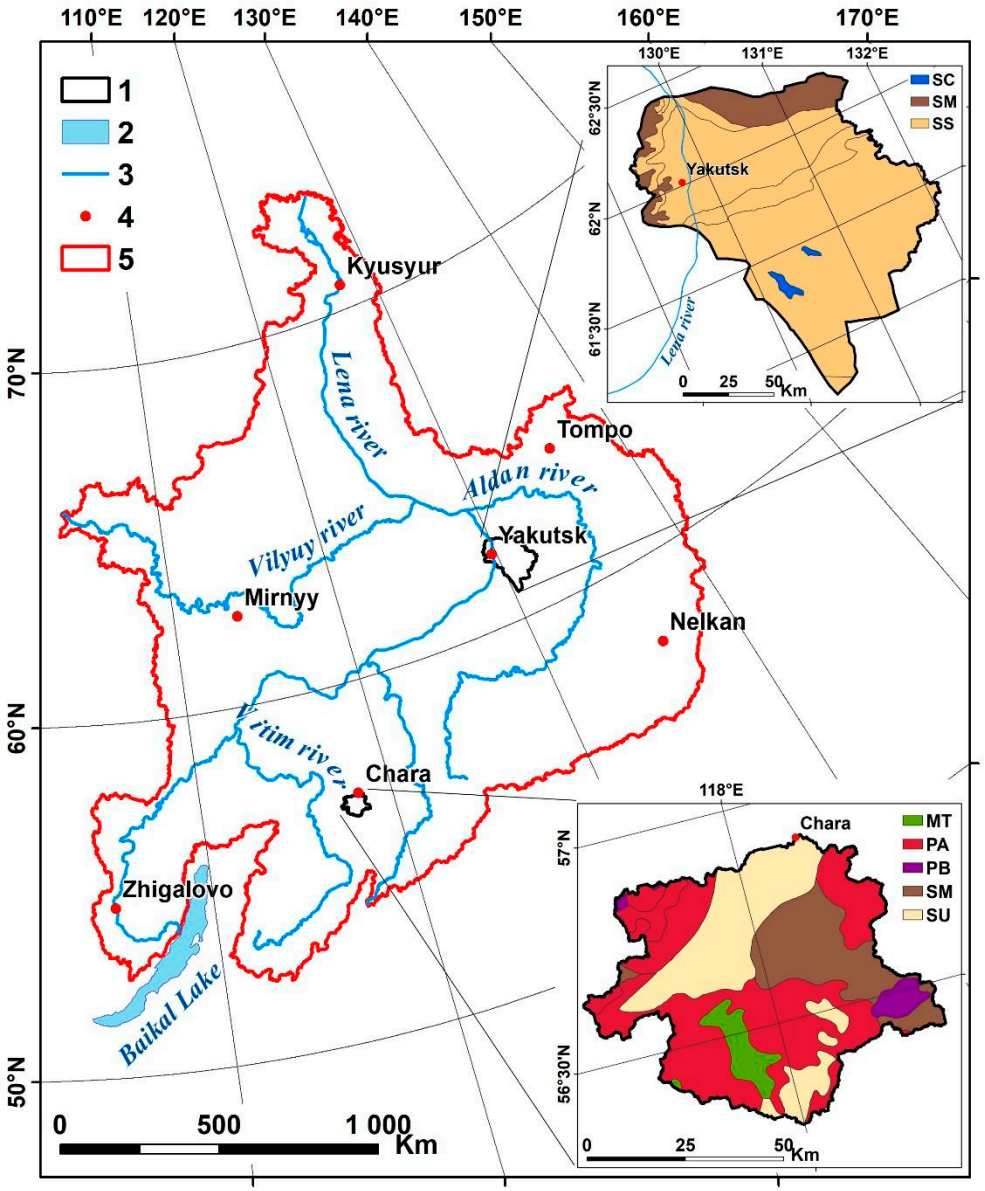

Figure 1. An overview map of the study area location: 1: borders of the study catchments; 2: lake; 3: main rivers; 4: cities; 5: border of the Lena catchment. Lithology: SC: Carbonate Sedimentary Rocks; SM: Mixed Sedimentary Rocks; SS: Siliciclastic Sedimentary Rocks; MT: Metamorphic Rocks; PA: Acid Plutonic Rocks; PB: Basic Plutonic Rocks; SU: Unconsolidated Sediments [37].

Table 1. The main natural characteristics of the studied areas.

Study Areas	Coordinates	Height a.s.l., m.	Mean Temperature 1966–2019, (°C)	Precipitation, mm (1966–2019)
«Chara»	56° 35′ n.l.; 117° 57′ e.l.	1449	−7	362
«Yakutsk»	61° 44′ n.l.; 130° 40′ e.l.	229	−8.86	237

The «Chara» catchment area is characterized by the values of the water surface runoff equal to 250 mm. The «Yakutsk» catchment area is characterized by the values of the water surface runoff equal to 50 mm [38].

These territories were chosen because we have data observation on the suspended sediments yield for them, which will allow us to conclude about the correctness of predicted calculations. These catchment areas are characterized by the environmental parameters presented in Table 1. It should be noted that despite the negative average annual temperatures, during May, June, July, August, and September positive temperatures are observed here, which allow the formation of surface runoff by rainfall precipitation. The soil cover is represented by the Lithic Leptosols Humic, Rustic Podzols, Histic Gleysols Dystric in the catchment area of the Chara River and Haplic Cambisoils Eutric, Haplic Cambisoils Distric, Rubic Arenosols Eutric, and Voronic Chernozems Pachic.

2.2. Method

The WaTEM/SEDEM model [13,14] was used for the average long-term assessment of the net erosion and sediment yield to the river network. Net erosion and accumulation maps were also created. The WaTEM/SEDEM is based on a raster model of spatial data. The main structural element of the raster model is a pixel or grid cell. The methodology consists of three steps. The first step is to estimate the potential soil loss within each grid pixel based on the revised universal soil loss equation (RUSLE) Equation (1) [5].

$$E = R \times K \times LS_{2D} \times C \times P \quad (1)$$

where E: the mean annual soil loss (kg m^{-2} $year^{-1}$), R: the rainfall erosivity factor (MJ mm m^{-2} h^{-1} $year^{-1}$), K: the soil erodibility (kg hour MJ^{-1} mm^{-1}), LS_{2D}: the slope length and steepness factor (dimensionless), C: the crop management factor (dimensionless), and P: the erosion control practice factor.

In the second stage, the transport of eroded material is simulated. Sediment movement is estimated until the river element is reached. The sediment transport is calculated using transport capacity (Equation (2)):

$$TC = ktc \times R \times K \times (LS_{2D} - 4.1 \times S_{IR}), \quad (2)$$

where TC is the transport capacity (kg m^{-2} $year^{-1}$), ktc: the transport capacity coefficient (m) depending on the type of land cover, S_{IR}: the interrill slope gradient factor, and the other variables are the same as in Equation (1).

The model uses two values of ktc: *ktchigh* for arable land; *ktclow* for unploughed land. We used the values of the coefficients set by default in the software package when modeling within the studied areas: *ktchigh* = 250, and *ktclow* = 75.

The routing algorithm was used to transfer the eroded sediment from the source to the river network at the third. The amount of sediment delivered from the up-slope areas was added to sediment produced by erosion (E) for each pixel. If the sum exceeded the transport capacity (TC) of the flow, then the sediment yield from the pixel was limited to the transport capacity. If the sum of the sediment delivered to a given grid pixel and the sediment formed by erosion in that pixel was lower than the transport capacity of the flow, then all the sediment was transported further down the slope.

The results of the model's work are a spatial model of net erosion; the average long-term mass of sediments load from the catchment area to the river network. The average long-term mass of sediments load obtained by the WaTEM/SEDEM was compared with measured values of suspended sediments at the gauging stations.

2.3. Input Data

The following cartographic models were used for calculations of sediment yield and net erosion maps within study areas: relief, soil erodibility; land use; rainfall erosivity factor; model of C-factor. A raster model for representing spatial data was used with grid pixel size (100 × 100 m) in our study.

2.3.1. Relief and LS-Factor

Currently, there are several free available global elevation models (DEM) representing the relief with different resolutions from 1–7.5″: SRTM C-SIR, SRTM X-SAR [39,40], ASTER GDEM v.2 [41]; ASTER GDEM v.3; ALOS3D30 [42]; ArcticDEM [43]; GMTED 2010 [44] and others. All the models described above are the result of remote sensing of the earth. Additionally, there is a DEM with middle spatial resolution. This DEM has a spatial resolution of 3″ (about 100 m) and is available for download at http://viewfinderpanoramas.org (accessed on 22 September 2022) [45]. This model was created by a group of authors based on several data sources: two open-source elevation models, the SRTM C-SIR and ASTER GDEM, as well as topographic maps at a scale of 1:100,000 and 1:200,000. This relief model was used because in the future we plan to conduct similar studies for the entire Lena River catchment (about 2.6 million km^2). Using a more detailed spatial resolution for such a vast area is difficult. The Nearing [3] method is used to assess the LS-factor in the WaTEM/SEDEM methodology in our study.

2.3.2. Soil Erodibility

The spatial and attributive data of the Unified State Register of Soil Resources of Russia (USRSR), the data which are presented on the website http://egrpr.esoil.ru/ (accessed on 22 September 2022), were used to create a spatial model of erodibility (K-factor). The USRSR was mainly created based on the soil map of scale 1:2,500,000 [46]. The soil erosion map was created with Formula 3 and initial data from USRSR. An alternative source of spatial soil data for this area is the Harmonized World Soil Database (HWSD) [47], as well as data from the SoilGrids project [48], which have a lower spatial resolution since they were created for this area based on more generalized soil maps.

$$K = \left(\frac{\left(2.1(d(100-e))^{1.14}\right)0.0001(12-a) + 3.25(b-2) + 2.5(c-3)}{100} \right) 0.1317 \quad (3)$$

where (a: soil organic matter (%), d: the fraction content of particles 0.002–0.1 mm in size (%), e: the fraction content of particles < 0.002 mm in size (%), b: the classes for structure and c: the classes of permeability). A more detailed description of the erodibility calculation is given in the USLE, RUSLE, and RUSLE2 models [4,5,49]. Maps of soil types of the studied areas are presented in Figures 2 and 3.

2.3.3. Land Use

The spatial land use model of the study areas was obtained on the GlobCover2009 land cover model [50] from which forests, meadows, and water bodies were identified. Anthropogenic objects (roads, settlements) and arable lands were recognized by us from the ESA WorldCover model [51], obtained using Sentinel high-resolution images.

The high-resolution satellite images presented in Google Earth for the modern period and images from the KeyHole-4B reconnaissance satellite (CORONA program) for the USSR period have been used to assess land-use dynamics. Eight KeyHole images covering the entire territory for the late 1960s with a spatial resolution of 1.8 m were selected for the "Yakutsk" catchment (Table 2).

It should be noted that data on sediment yield is for the 1966–1985 period, but are KeyHole images for the end of the 60s. However, due to the cropland area dynamics during the Soviet period being very insignificant [52], using the mentioned images for the 1966–1985 period seems acceptable for our aim.

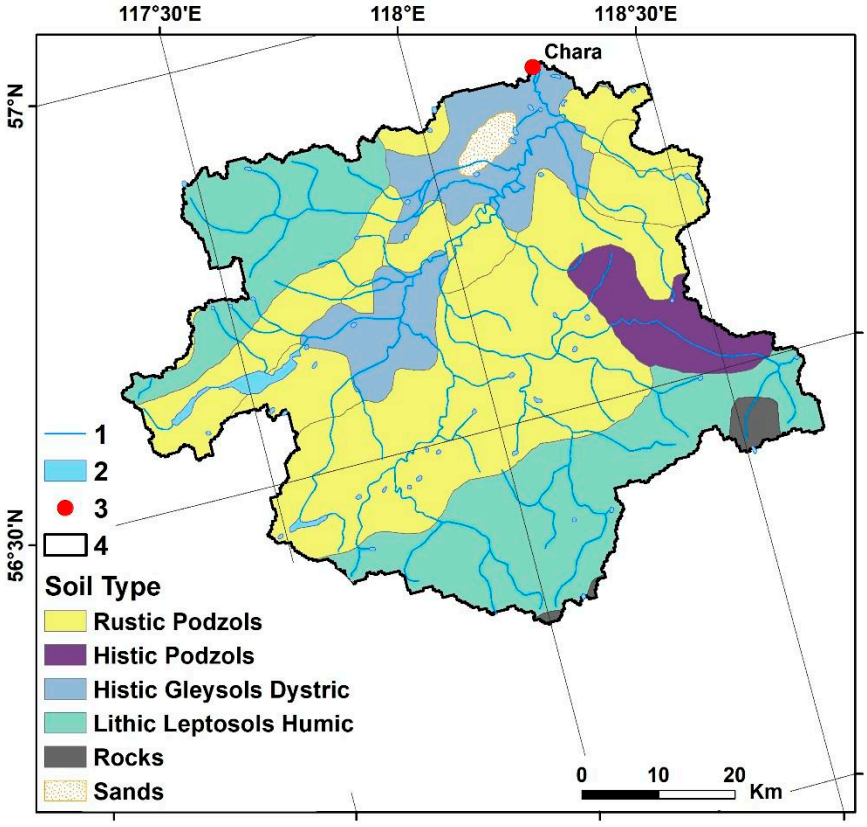

Figure 2. Soil types of the Chara study area (1: rivers, 2: lakes, 3: settlement, 4: catchment area).

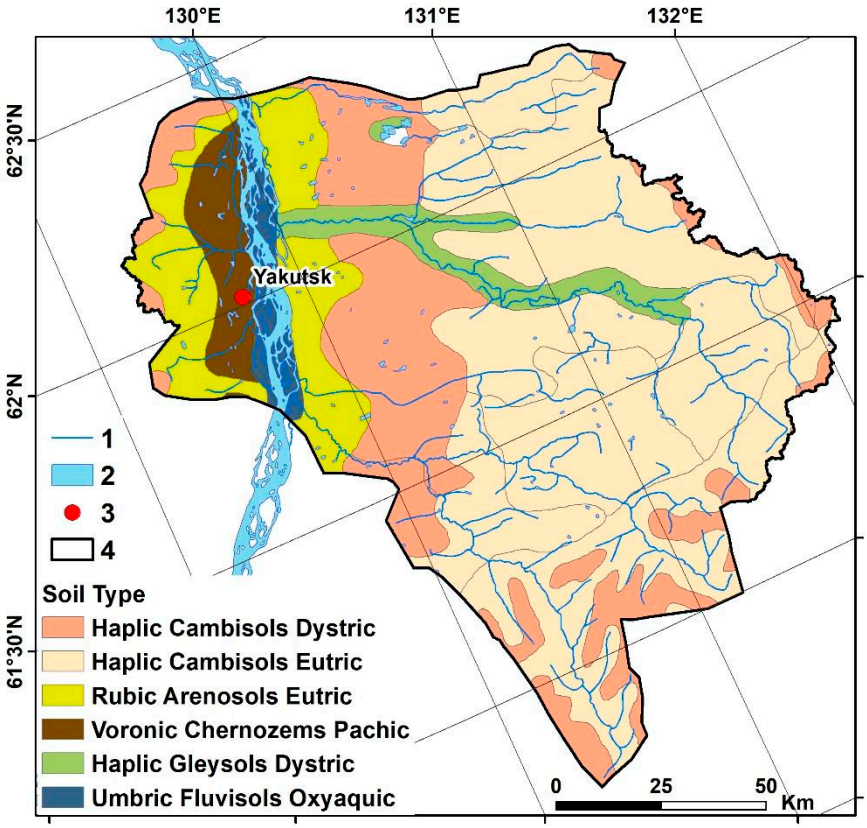

Figure 3. Soil types of the Yakutsk study area (1: rivers, 2: Lena iver and lakes, 3: settlement, 4: catchment area).

Table 2. Used KeyHole-4B images.

Scene ID	Date	Mission
DS1107–2246DA002	08 August 1969	1107–2
DS1107–2246DA003		
DS1107–2246DA004		
DS1101–1068DA040	20 September 1967	1101–1
DS1101–1068DA041		
DS1101–1068DA042		
DS1101–1068DA043		
DS1101–1068DA044		

The Georeferencing module in ArcGIS was used to geo-reference the KeyHole images (projection WGS 84/UTM 50 Northern Hemisphere). Modern (2018–2021) very high-resolution satellite images were used as reference data. These images are available as global base maps from Google and ESRI in the QGIS module: HCMGIS. Crossroads and unchanged objects (buildings, logging sites) were chosen as reference points. The third-order polynomial transformation and bilinear interpolation were used. The maximum georeferencing errors for all images were less than 6 pixels [53].

Cultivated cropland was recognized in modern images by several features: orthogonal boundaries, homogeneous tone, texture (furrows from plowing), and the presence of protective forest lines at the field boundaries (Figure 4a). At the same time, the crop field plowed for at least one year in the period 2019–2021 was recognized as cultivated. Abandoned cropland is also quite easily identified by overgrown grass (spotted pattern), shrubs, and trees. Sometimes fields are partially flooded (Figure 4b). Due to the lack of multi-temporal data, croplands for the Soviet period were recognized by the general features listed above, except color, since the KeyHole images are black and white (Figure 4c).

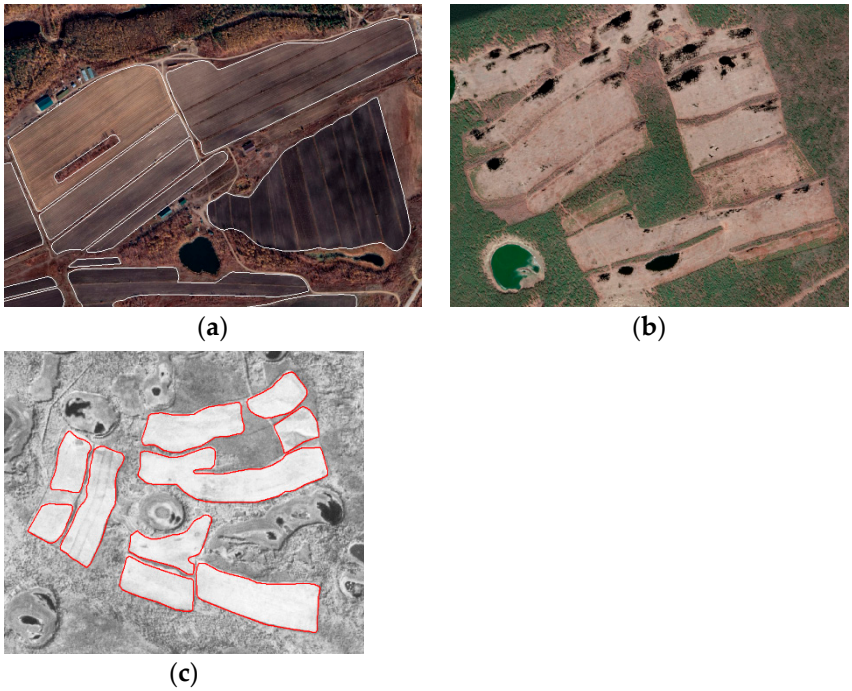

Figure 4. Modern cultivated cropland on the high-resolution images (**a**), Abandoned crop fields (**b**), and cultivated cropland in 1969 (**c**).

The modern crop fields were digitized manually and overlaid onto the KeyHole images. Boundaries were corrected, and the remaining fields were digitized. In some cases, crop fields look pretty similar to logging sites; therefore, modern images were used as auxiliary data. If an unclear area is an abandoned field in the modern image, it was identified as a cultivated field for the Soviet period. Thus, vector layers of cropland for two periods were obtained (Figure 5).

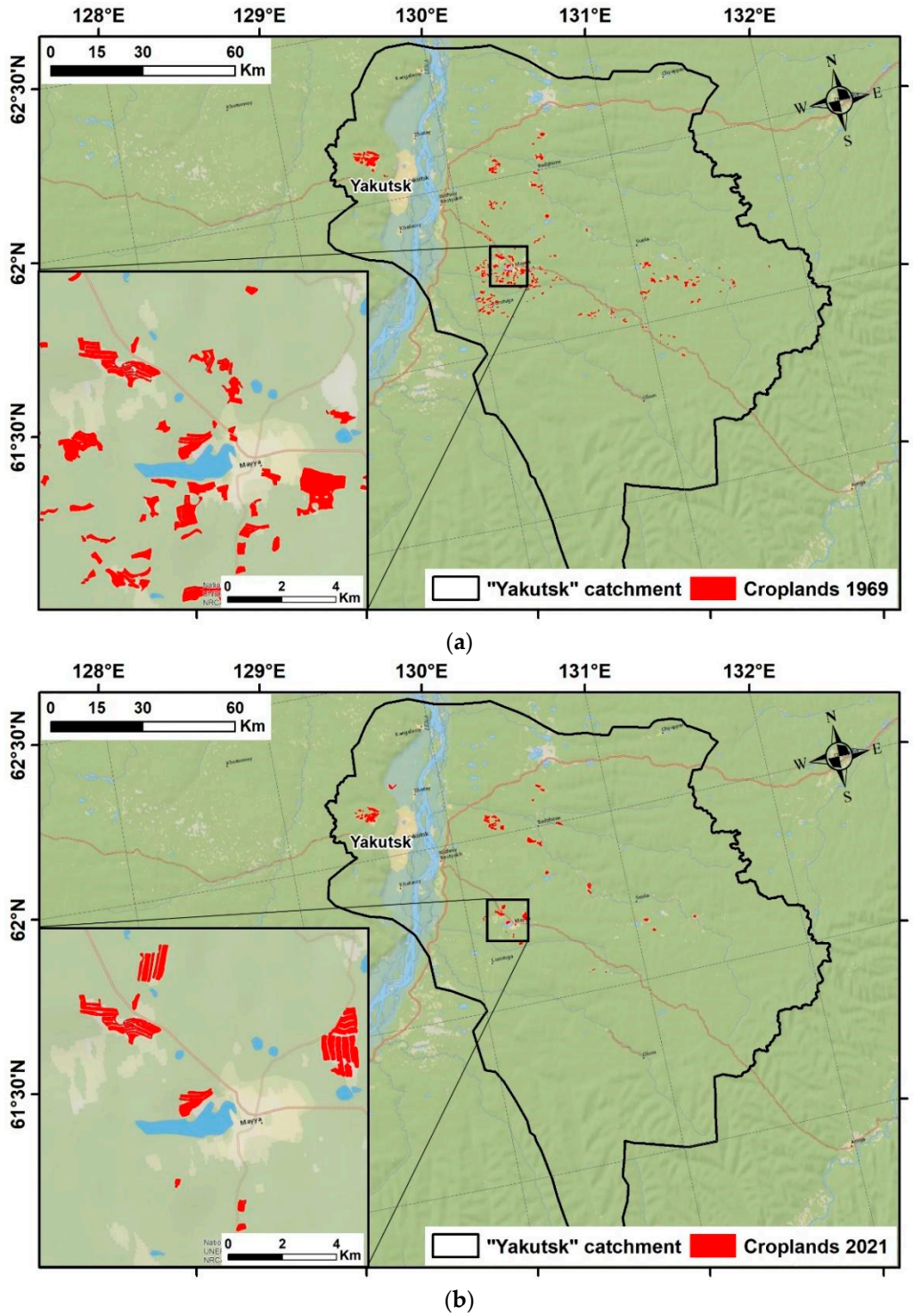

Figure 5. Maps of cropland allocation for two considering periods ((**a**): croplands 1969; (**b**): croplands 2021).

The cropland area was calculated, amounting to 6718.5 ha in 1969 and 3337.2 ha in 2021, i.e., 0.42% and 0.21% of the total catchment area. It should be noted that with a general decrease in area, in some places the plowing of new sites is observed. Despite the almost twofold reduction in the area of arable land, its insignificant share of the total catchment area allows us to conclude that its contribution to the suspended sediment yield formation is none.

There are no arable lands at all, but there is mining from a quarry within the «Chara» area. The impact of quarries on the sediment yield formation proved impossible to assess due to the lack of good coverage of the Chara River catchment with high-resolution images. It is very difficult to recognize quarries from lower-resolution images due to their small size. However, the share of the area occupied by quarries is still an order lower than by cropland. Therefore, their contribution seems insignificant to us. Therefore, we can use one land use model for the two considered periods (1966–1985; 1986–2019) obtained based on the GlobCover2009 land cover model [50] and ESA WorldCover model [51].

The WaTEM/SEDEM methodology requires not only a spatial model of land use but also a spatial model of the C-factor. Based on the created land use models and C-factor value proposed by P. Panagos [54] and L.F. Litvin [55], the C-factor spatial models were also created for the study areas seen in Table 3.

Table 3. Land use/land cover and their C-factor value.

Land Use/Land Cover	C-Factor Value
Forest	0.003
Meadows	0.1
Arable lands	0.36
Anthropogenic objects (roads, settlements)	0.03
Water bodies	0

2.3.4. Precipitation

The spatial model of the rainfall erosivity factor obtained in the study [56] was used as a basis to perform this work. The initial data on the intensity of rainfall for the period from 1961–1984 was used for the territory of Russia. Over the past few decades, starting from 1985–1990, an intensification of climate change was noted by many authors [57,58], expressed in a change in the amount of precipitation and the intensity of the precipitation. Unfortunately, there is no modern data on the intensity of precipitation in the study area; therefore, we analyzed the change in the amount of precipitation within the studied catchment area. Further, based on the obtained changes, the used model [56] was corrected for the time interval 1986–2019.

Analysis of data from the Russian Research Institute of Hydrometeorological Information: World Data Center website, meteo.ru, shows a slight increase in the average long-term annual precipitation in the catchment area of the Chara River from 357 mm (average for 1966–1985) to 400 mm (average for 1986–2019). The increase in average annual precipitation is due to an increase in rainfall precipitation from 287 mm to 337 mm (an increase of 15%). The snow precipitation decreased from 59 to 46 mm per year.

The analysis of changes in the amount of precipitation within the "Yakutsk" catchment area shows a much smaller change in the above time intervals, both for average annual and rainfall precipitation. The average long-term precipitation for the same time intervals is 241 mm and 240 mm, and the amount of rainfall precipitation is 162 and 163 mm. The amount of snow precipitation here is 79 mm and 77 mm. It can be stated that there is almost no change in the amount of precipitation in this area.

3. Results

It was found that for the period from 1966–1985 the total average annual mass of sediments loaded in the river network from the catchment area of the Chara River is predicted at 616,000 tons (Table 4). The specific sediment yield here is 149 t/km^2 per year. A 15% increase in precipitation between the 1966–1985 and 1986–2019 time intervals should result in an increase in sediment load to 717,000 t/year into the river network or a specific sediment yield of 172 t/km^2 per year.

Table 4. Predicted values of sediment yield in rivers from the territory of the study areas.

Study Area	1966–1985 Years		1986–2019 Years	
«Chara»	616,000 t/year	149 t/km^2 per year	717,000 t/year	172 t/km^2 per year
«Yakutsk»	50,073 t/year	3.5 t/km^2 per year	50,073 t/year	3.5 t/km^2 per year

An analysis of the predicted sediment yield from the catchment area to the rivers within the "Yakutsk" catchment area indicates 50,073 tons per year or a specific sediment yield of 3.5 t/km^2 per year. Sediment yield from the "Yakutsk" catchment area has not changed from 1966–1985 to the 1986–2019 time interval, according to predicted data.

A comparative analysis was carried out of predicted data of sediment yield from the catchment area to rivers with data measured at gauging stations of the national monitoring network of Russia. The predicted data are very different from the sediment yield measured at the gauging station of the Chara River according to our study. The predicted values show an increase in sediment yield values. The sediment yield of the Chara River from the 1966–1985 to 1986–2019 periods decreased from 28 to 15 t/km^2 per year, while maintaining constant water discharge according to D.V. Magritsky and L.S. Banshchikov [59]. Comparing these data with the simulation data in Table 4, we see that not only do the values differ, but also the direction of their change.

There can be few explanations for the contradictions. Firstly, this can be explained by the fact that those transport capacity coefficients that are set in the WaTEM/SEDEM model by default need to be calibrated when working within the mountain catchment area we are considering. However, in this study, this cannot be done due to the lack of data necessary for calibration.

Secondly, the sediment yield from the territory of the mountain catchment area can be implemented due to a larger proportion of large particles that accumulate in the channel and do not reach the measurement station, and those sediments that reach are transported in the form of bed loads and are not taken into account at the measurement station.

Thirdly, lakes Leprindo and Leprindokan, located in the riverbed, can act as large traps for sediments that can trap a significant part of the sediment.

A comparative analysis of the data of simulation of sediment yield from the "Yakutsk" catchment area shows good agreement with the measured data at the Tabaga gauging station. The sediment yield from river catchment areas in this area is 3.5 t/km^2 per year and, according to our estimates, has not changed over the past 34 years. The sediment yield measured in the river is 7.08 t/km^2 according to data from 1966–1985 and 9.45 t/km^2 per year according to data measured in the interval 1986–2019 [59].

Net Erosion Maps Analysis

The maps of net erosion, which represent the erosion-accumulation budget of the studied areas, are an additional result of this work. Such maps were created for the period 1985–2019. The entire territory of the studied part of the catchment area of the Chara River is characterized by soil erosion losses of 1.72 t/ha per year in the period from 1986–2019. The gross soil erosion is about 17 t/ha per year. Soil erosion occurs within 96% of the Chara catchment area according to predicted data. Large erosion values in the catchment are generally located on steep slopes in the upper reaches of the Chara tributaries. The

accumulation of part of the eroded material occurs in a small part of the study area (4%) at the foot of steep slopes, in river valleys within the dry valley, and is characterized by high rates, on average, up to −390 t/ha per year (Figure 6).

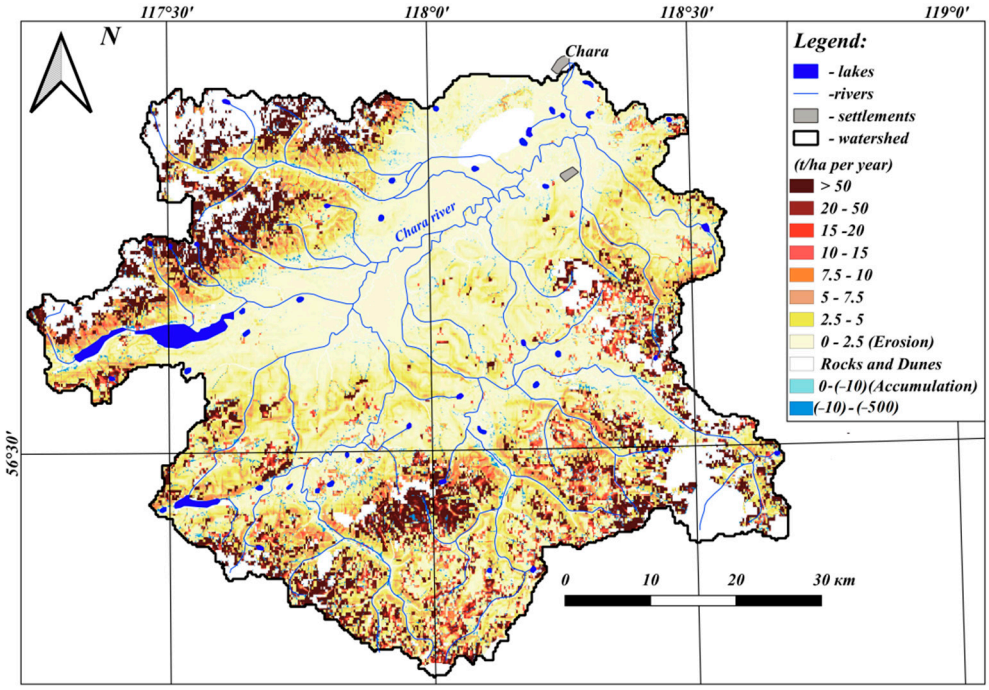

Figure 6. A spatial model of net water erosion in the catchment of the river Chara (1986–2019 period).

The "Yakutsk" study area is characterized by very small values of soil erosion loss, averaging at 0.035 t/ha per year in the period from 1985–2019. This value of erosion is typical for the whole catchment area and was obtained from the accumulation of part of the eroded material within the catchment area. The gross soil erosion is about 0.1 t/ha per year. Soil erosion occurs within 98% of the area of this catchment area according to predicted data. High values of erosion in the catchment area most often correspond to the steep left slope of the Lena River. In addition, relatively high values of soil erosion losses are typical for the right banks of the tributaries of the Lena River (Figure 7). The accumulation of part of the eroded material occurs in a small part of the study area (2%) and is characterized by an average value of −2.5 t/ha per year.

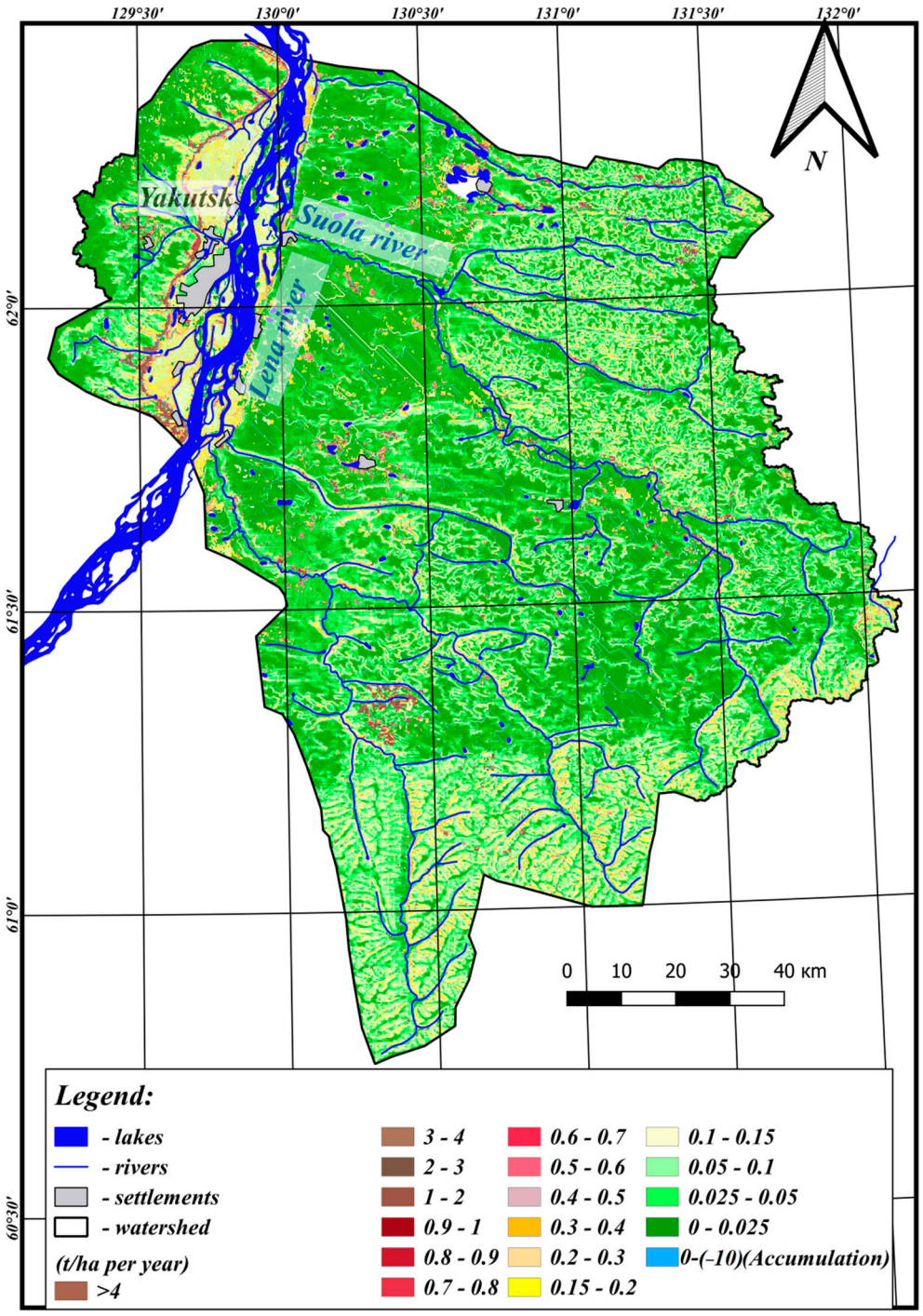

Figure 7. A spatial model of net water erosion of the «Yakutsk» catchment area (1986–2019 period).

4. Discussion

The "Yakutsk" catchment area has repeatedly become the subject of a study on the assessment of gross erosion as part of larger-scale work. Therefore, we compared the values of gross erosion obtained by us and the results of previous studies (Table 5).

Analysis of Table 4 shows that different results were obtained, and some estimates differ by more than three times.

Table 5. Gross erosion values (t/ha per year).

	Average (t/ha Per Year)
WaTEM/Sedem	0.1
Shynbergenov and Yermolaev, 2017 [21]	0.047
Chalov et. al., 2021 [60]	0.03
Borrelli et al., 2017 [22]	0–1

These differences can be explained by a few reasons. These differences can be explained by the scale of the study. For example, this study was performed using a raster model with a grid pixel size of 100 m, and the study by authors [21] was performed using a grid pixel size of 250 m. The model proposed by Moscow State University [61] is used instead of the RUSLE model in the same study [21]. The differences between the estimates obtained in this study and the study of S.R. Chalov [60] can be explained by the differences associated with the use of initial data on soil erodibility

Thus, S.R. Chalov's study uses the base to calculate the erodibility by HWSD v 1.2 (Harmonized World Soil Database, created by FAO, Rome, Italy and IIASA, Laxenburg, Austria) [62]. For example, the entire Yakutsk site has the same erodibility value using HWSD, whereas the use of the initial data of the USRSR shows that several types of soils prevail within the Yakutsk site, which is very different in terms of erodibility due to different soil organic matter content and different granulometric composition.

Studies obtaining net erosion maps of the annual erosion–accumulation budget of deposits are rare. For example, the USPED model allows erosion and accumulation maps for Washington State (USA) [63]. However, only qualitative analysis was conducted in this study, and there are no quantitative estimates of the sediment budget. Six categories of land characterized by erosion/accumulation were identified: three categories of erosion and three categories of accumulation.

The quantitative spatial model of the erosion–accumulation budget has been created within 68 river catchments in Spain using the WaTEM/SEDEM model [33,64]. For example, the WaTEM/SEDEM was used for net erosion map creation within the catchment of the Taibilla reservoir with a mountainous relief given in a study [33]. The erosion intensity within the Taibilla basin is equal to a maximum of 20 t/ha per year, which is comparable to the rates for the Chara River basin (17 t/ha per year). At the same time, the intensity of accumulation in these two basins is quite different.

A net water erosion map using the WaTEM/SEDEM model was constructed in Mongolia in analyzing the contribution of gold mines to the sediment yield of the Tuul River [35]. Although the model WaTEM/SEDEM allows us to obtain quantitative values of erosion/accumulation, the authors of the study [35] do not give them but present only five categories: deposition, low erosion, moderate erosion, high erosion, and very high erosion.

Studies using the model WaTEM/SEDEM were carried out within China, in the Shuangfengtan catchment [32]. The study also assessed the feasibility of using the WaTEM/SEDEM model to predict sediment yield from the catchment area. A quantitative map of the erosion/accumulation budget was obtained. The erosion values are a maximum of 80 t/ha per year, which is much more than the erosion values obtained by us.

5. Conclusions

The analysis was made of the possibility of assessing the sediment yield and its dynamics using the WaTEM/SEDEM model within two catchment areas located in the Lena River catchment and differing in relief conditions in this study. The analysis was performed based on a comparison of simulation data and observed data.

It was found the simulated sediment yield significantly exceeds (172 t/km^2 per year from 1986–2019) the observed values of suspended sediment yield (15 t/km^2 per year) at the gauging station within the mountain catchment area of the Chara River. The predicted

data have inverse temporal dynamics compared to the measured sediment yield at the gauging station. The simulation results within the Yakutsk catchment area, which is located within the plain territory, are better consistent with the measurement data at gauging stations, both in absolute values and in their dynamics over the past few decades. The model sediment yield from the study area has not changed and is 3.5 t/km^2, while the suspended sediment yield in the Lena at the Tabaga post slightly increased from 7 t/km^2 to 9.45 t/km^2 per year from 1966–1985 to 1986–2019.

An analysis of the obtained maps shows that more than 96% of the considered catchment areas are subject to erosion processes, and the accumulation processes happen in less than 4% of the area. An analysis of the values of gross and net erosion in the considered catchment areas shows that most of the eroded material remains within the catchment areas.

Author Contributions: Conceptualization, K.M.; methodology, K.M.; validation, M.I.; investigation, K.M.; resources, M.I.; data curation, M.I.; writing—original draft preparation, K.M., M.I.; writing—review and editing, K.M.; visualization, K.M. and M.I. All authors have read and agreed to the published version of the manuscript.

Funding: The study was carried out with the support of the Russian Science Foundation project 22-17-00025—preparation and analysis of data; the Russian Science Foundation project 21-17-00181 mathematical and statistical data processing; the Kazan Federal University Strategic Academic Leadership Program ("PRIORITY-2030")—working methodology and software.

Institutional Review Board Statement: Not applicable.

Informed Consent Statement: Not applicable.

Data Availability Statement: Not applicable.

Conflicts of Interest: The authors declare no conflict of interest.

References

1. Nummelin, A.; Ilicak, M.; Li, C.; Smedsrud, L.H. Consequences of Future Increased Arctic Runoff on Arctic Ocean Stratification, Circulation, and Sea Ice Cover. *J. Geophys. Res. Ocean.* **2016**, *121*, 617–637. [CrossRef]
2. Borrelli, P.; Alewell, C.; Alvarez, P.; Anache, J.A.A.; Baartman, J.; Ballabio, C.; Bezak, N.; Biddoccu, M.; Cerdà, A.; Chalise, D.; et al. Soil Erosion Modelling: A Global Review and Statistical Analysis. *Sci. Total Environ.* **2021**, *780*, 146494. [CrossRef] [PubMed]
3. Nearing, M.A. A Single, Continuous Function for Slope Steepness Influence on Soil Loss. *Soil Sci. Soc. Am. J.* **1997**, *61*, 917–919. [CrossRef]
4. Wischmeier, W.H.; Smith, D.D. *Predicting Rainfall Erosion Losses: A Guide to Conservation Planning*; USDA: Hyattsville, MD, USA, 1978; p. 67.
5. Renard, K.G.; Foster, G.R.; Weesies, G.A.; McCool, D.K. Predicting Soil Erosion by Water: A Guide to Conservation Planning with the Resived Universal Soil Loss Equation (RUSLE). In *Agriculture Handbook*; SSOP: Washington, DC, USA, 1997; ISBN 0-16-048938-5.
6. Kumar, P.S.; Praveen, T.V.; Prasad, M.A. Simulation of Sediment Yield Over Un-Gauged Stations Using MUSLE and Fuzzy Model. *Aquat. Procedia* **2015**, *4*, 1291–1298. [CrossRef]
7. Kandel, D.D.; Western, A.W.; Grayson, R.B. Scaling from Process Timescales to Daily Time Steps: A Distribution Function Approach. *Water Resour. Res.* **2005**, *41*, 1–16. [CrossRef]
8. Pieri, L.; Bittelli, M.; Wu, J.Q.; Dun, S.; Flanagan, D.C.; Pisa, P.R.; Ventura, F.; Salvatorelli, F. Using the Water Erosion Prediction Project (WEPP) Model to Simulate Field-Observed Runoff and Erosion in the Apennines Mountain Range, Italy. *J. Hydrol.* **2007**, *336*, 84–97. [CrossRef]
9. Grum, B.; Woldearegay, K.; Hessel, R.; Baartman, J.E.M.; Abdulkadir, M.; Yazew, E.; Kessler, A.; Ritsema, C.J.; Geissen, V. Assessing the Effect of Water Harvesting Techniques on Event-Based Hydrological Responses and Sediment Yield at a Catchment Scale in Northern Ethiopia Using the Limburg Soil Erosion Model (LISEM). *CATENA* **2017**, *159*, 20–34. [CrossRef]
10. Schob, A.; Schmidt, J.; Tenholtern, R. Derivation of Site-Related Measures to Minimise Soil Erosion on the Watershed Scale in the Saxonian Loess Belt Using the Model EROSION 3D. *CATENA* **2006**, *68*, 153–160. [CrossRef]
11. Morgan, R.P.C.; Quinton, J.N.; Smith, R.E.; Govers, G.; Poesen, J.W.A.; Auerswald, K.; Chisci, G.; Torri, D.; Styczen, M.E. The European Soil Erosion Model (EUROSEM): A Dynamic Approach for Predicting Sediment Transport from Fields and Small Catchments. *Earth Surf. Process. Landf.* **1998**, *23*, 527–544. [CrossRef]
12. Merritt, W.S.; Letcher, R.A.; Jakeman, A.J. A Review of Erosion and Sediment Transport Models. *Environ. Model. Softw.* **2003**, *8–9*, 761–799. [CrossRef]

13. Van Rompaey, A.J.J.; Verstraeten, G.; Van Oost, K.; Govers, G.; Poesen, J. Modelling Mean Annual Sediment Yield Using a Distributed Approach. *Earth Surf. Process. Landf.* **2001**, *26*, 1221–1236. [CrossRef]
14. Verstraeten, G.; Prosser, I.P.; Fogarty, P. Predicting the Spatial Patterns of Hillslope Sediment Delivery to River Channels in the Murrumbidgee Catchment, Australia. *J. Hydrol.* **2007**, *334*, 440–454. [CrossRef]
15. Dabney, S.M.; Yoder, D.C.; Vieira, D.A.N. The Application of the Revised Universal Soil Loss Equation, Version 2, to Evaluate the Impacts of Alternative Climate Change Scenarios on Runoff and Sediment Yield. *J. Soil Water Conserv.* **2012**, *67*, 343–353. [CrossRef]
16. Morgan, R.P.C.; Morgan, D.; Finney, H.J. A Predictive Model for Assessment of Erosion Risk. *J. Agric. Eng. Res.* **1984**, *30*, 245–253. [CrossRef]
17. Arnold, J.; Moriasi, D.; Gassman, P.; Mikayilov, F.; White, M.; Srinivasan, R.; Santhi, C.; Harmel, R.; van Griensven, A.; Van Liew, M.; et al. SWAT: Model Use, Calibration, and Validation. *Trans. ASABE* **2012**, *55*, 1491–1508. [CrossRef]
18. Vigiak, O.; Malagó, A.; Bouraoui, F.; Vanmaercke, M.; Poesen, J. Adapting SWAT Hillslope Erosion Model to Predict Sediment Concentrations and Yields in Large Basins. *Sci. Total Environ.* **2015**, *538*, 855–875. [CrossRef]
19. Ryzhov, Y.V. The Erosion-Accumulative Processes within the Basins of Small Rivers of Southern East Siberia. *Geogr. Nat. Resour.* **2009**, *30*, 265–271. [CrossRef]
20. Litvin, L.F.; Kiryukhina, Z.P.; Krasnov, S.F.; Dobrovol'skaya, N.G.; Gorobets, A.V. Dynamics of Agricultural Soil Erosion in Siberia and Far East. *Eurasian Soil Sci.* **2021**, *54*, 150–160. [CrossRef]
21. Shynbergenov, E.A.; Yermolaev, O.P. Potential Soil Erosion in the Lena River Basin. *Bull. Udmurt Univ. Ser. Biol. Earth Sci.* **2017**, *27*, 513–528. (In Russian)
22. Borrelli, P.; Robinson, D.A.; Fleischer, L.R.; Lugato, E.; Ballabio, C.; Alewell, C.; Meusburger, K.; Modugno, S.; Schütt, B.; Ferro, V.; et al. An Assessment of the Global Impact of 21st Century Land Use Change on Soil Erosion. *Nat. Commun.* **2017**, *8*, 2013. [CrossRef]
23. Boomer, K.B.; Weller, D.E.; Jordan, T.E. Empirical Models Based on the Universal Soil Loss Equation Fail to Predict Sediment Discharges from Chesapeake Bay Catchments. *J. Environ. Qual.* **2008**, *37*, 79–89. [CrossRef] [PubMed]
24. Baartman, J.E.M.; Masselink, R.; Keesstra, S.D.; Temme, A.J.A.M. Linking Landscape Morphological Complexity and Sediment Connectivity: Landscape Morphological Complexity and Sediment Connectivity. *Earth Surf. Process. Landf.* **2013**, *38*, 1457–1471. [CrossRef]
25. Heckmann, T.; Cavalli, M.; Cerdan, O.; Foerster, S.; Javaux, M.; Lode, E.; Smetanová, A.; Vericat, D.; Brardinoni, F. Indices of Sediment Connectivity: Opportunities, Challenges and Limitations. *Earth-Sci. Rev.* **2018**, *187*, 77–108. [CrossRef]
26. Borselli, L.; Cassi, P.; Torri, D. Prolegomena to Sediment and Flow Connectivity in the Landscape: A GIS and Field Numerical Assessment. *CATENA* **2008**, *75*, 268–277. [CrossRef]
27. Gay, A.; Cerdan, O.; Mardhel, V.; Desmet, M. Application of an Index of Sediment Connectivity in a Lowland Area. *J. Soils Sediments* **2016**, *16*, 280–293. [CrossRef]
28. Zhao, G.; Gao, P.; Tian, P.; Sun, W.; Hu, J.; Mu, X. Assessing Sediment Connectivity and Soil Erosion by Water in a Representative Catchment on the Loess Plateau, China. *CATENA* **2020**, *185*, 104284. [CrossRef]
29. Ferro, V.; Porto, P. Sediment Delivery Distributed (SEDD) Model. *J. Hydrol. Eng.* **2000**, *5*, 411–422. [CrossRef]
30. Bhattarai, R.; Dutta, D. A Comparative Analysis of Sediment Yield Simulation by Empirical and Process-Oriented Models in Thailand/Une Analyse Comparative de Simulations de l'exportation Sédimentaire En Thaïlande à l'aide de Modèles Empiriques et de Processus. *Hydrol. Sci. J.* **2008**, *53*, 1253–1269. [CrossRef]
31. Zhidkin, A.P.; Smirnova, M.A.; Gennadiev, A.N.; Lukin, S.V.; Zazdravnykh, Y.A.; Lozbenev, N.I. Digital Mapping of Soil Associations and Eroded Soils (Prokhorovskii District, Belgorod Oblast). *Eurasian Soil Sci.* **2021**, *54*, 13–24. [CrossRef]
32. Sheng, M.; Fang, H. Research Progress in WaTEM/SEDEM Model and Its Application Prospect. *Prog. Geogr.* **2014**, *33*, 85–91. [CrossRef]
33. de Vente, J.; Poesen, J.; Verstraeten, G.; Van Rompaey, A.; Govers, G. Spatially Distributed Modelling of Soil Erosion and Sediment Yield at Regional Scales in Spain. *Glob. Planet. Chang.* **2008**, *60*, 393–415. [CrossRef]
34. Van Rompaey, A.; Bazzoffi, P.; Jones, R.; Montanarella, L. Modeling Sediment Yields in Italian Catchments. *Geomorphology* **2005**, *65*, 157–169. [CrossRef]
35. Pietroń, J.; Chalov, S.R.; Chalova, A.S.; Alekseenko, A.V.; Jarsjö, J. Extreme Spatial Variability in Riverine Sediment Load Inputs Due to Soil Loss in Surface Mining Areas of the Lake Baikal Basin. *Catena* **2017**, *152*, 82–93. [CrossRef]
36. Maltsev, K.; Golosov, V.; Yermolaev, O.; Ivanov, M.; Chizhikova, N. Assessment of Net Erosion and Suspended Sediments Yield within River Basins of the Agricultural Belt of Russia. *Water* **2022**, *14*, 2781. [CrossRef]
37. Hartmann, J.; Moosdorf, N. The New Global Lithological Map Database GLiM: A Representation of Rock Properties at the Earth Surface. *Geochem. Geophys. Geosyst.* **2012**, *13*, Q12004. [CrossRef]
38. Kotljakov, V.M. (Ed.) *National Atlas of Russia. Volume 2: Nature. Ecology*; Roskartografija: Moscow, Russia, 2007; ISBN 978-5-85120-250-6. (In Russian)
39. Farr, T.G.; Rosen, P.A.; Caro, E.; Crippen, R.; Duren, R.; Hensley, S.; Kobrick, M.; Paller, M.; Rodriguez, E.; Roth, L.; et al. The Shuttle Radar Topography Mission. *Rev. Geophys.* **2007**, *45*, RG2004. [CrossRef]
40. Shortridge, A.; Messina, J. Spatial Structure and Landscape Associations of SRTM Error. *Remote Sens. Environ.* **2011**, *115*, 1576–1587. [CrossRef]

41. Reuter, H.I.; Neison, A.; Strobl, P.; Mehl, W.; Jarvis, A. A First Assessment of Aster GDEM Tiles for Absolute Accuracy, Relative Accuracy and Terrain Parameters. In Proceedings of the 2009 IEEE International Geoscience and Remote Sensing Symposium, Cape Town, South Africa, 12–17 July 2009; pp. V-240–V-243.
42. Tadono, T.; Ishida, H.; Oda, F.; Naito, S.; Minakawa, K.; Iwamoto, H. Precise Global DEM Generation by ALOS PRISM. *ISPRS Ann. Photogramm. Remote Sens. Spat. Inf. Sci.* **2014**, *4*, 71–76. [CrossRef]
43. Porter, C.; Morin, P.; Howat, I.; Noh, M.-J.; Bates, B.; Peterman, K.; Keesey, S.; Schlenk, M.; Gardiner, J.; Tomko, K.; et al. ArcticDEM. 2018. Available online: https://www.pgc.umn.edu/data/arcticdem/ (accessed on 22 September 2022).
44. Ermolaev, O.P.; Mal'tsev, K.A.; Mukharamova, S.S.; Kharchenko, S.V.; Vedeneeva, E.A. Cartographic Model of River Basins of European Russia. *Geogr. Nat. Resour.* **2017**, *38*, 131–138. [CrossRef]
45. Melkonian, A.K.; Willis, M.J.; Pritchard, M.E.; Stewart, A.J. Recent Changes in Glacier Velocities and Thinning at Novaya Zemlya. *Remote Sens. Environ.* **2016**, *174*, 244–257. [CrossRef]
46. Rukhovich, D.I.; Wagner, V.B.; Vil'chevskaya, E.V.; Kalinina, N.V.; Koroleva, P.V. Problems of Using Digitized Thematic Maps on the Territory of the Former Soviet Union upon the Creation of the "Soils of Russia" Geographic Information System. *Eurasian Soil Sci.* **2011**, *44*, 957–968. [CrossRef]
47. Fischer, G.; Nachtergaele, F.; Prieler, S.; van Velthuizen, H.; Verelst, L.; Wiberg, D. *Global Agro-Ecological Zones Assessment for Agriculture (GAEZ 2008)*; IIASA: Laxenburg, Austria; FAO: Rome, Italy, 2008.
48. Hengl, T.; Mendes de Jesus, J.; Heuvelink, G.B.M.; Ruiperez Gonzalez, M.; Kilibarda, M.; Blagotić, A.; Shangguan, W.; Wright, M.N.; Geng, X.; Bauer-Marschallinger, B.; et al. SoilGrids250m: Global Gridded Soil Information Based on Machine Learning. *PLoS ONE* **2017**, *12*, e0169748. [CrossRef]
49. Renard, K.G.; Yoder, D.C.; Lightle, D.T.; Dabney, S.M. Universal Soil Loss Equation and Revised Universal Soil Loss Equation. In *Handbook of Erosion Modelling*; Morgan, R.P.C., Nearing, M.A., Eds.; Wiley: Hoboken, NJ, USA, 2010; pp. 135–167, ISBN 978-1-4051-9010-7.
50. Arino, O.; Ramos Perez, J.J.; Kalogirou, V.; Bontemps, S.; Defourny, P.; Van Bogaert, E. Global Land Cover Map for 2009 (GlobCover 2009) 2012, 40 Data Points. Available online: https://doi.pangaea.de/10.1594/PANGAEA.787668 (accessed on 22 September 2022).
51. Zanaga, D.; Van De Kerchove, R.; De Keersmaecker, W.; Souverijns, N.; Brockmann, C.; Quast, R.; Wevers, J.; Grosu, A.; Paccini, A.; Vergnaud, S.; et al. *ESA WorldCover 10 m 2020 V100*; Zenodo: Geneve, Switzerland, 2021; Available online: https://esa-worldcover.org/en/data-access (accessed on 22 September 2022).
52. Lyuri, D.I.; Goryachkin, S.V.; Karavaeva, N.A.; Denisenko, E.A.; Nefedova, T.G. *Dynamics of Agricultural Lands in Russia in the XX Century and the Postagrogenic Restoration of Vegetation and Soils*; GEOS: Moscow, Russia, 2010; ISBN 978-5-89118-500-5. (In Russian)
53. Usmanov, B.M.; Gainullin, I.; Gafurov, A.M.; Rudenko, K.A.; Ivanov, M.A. Using Multitemporal Remote Sensing Data for Evaluation of the Kuibyshev Reservoir Bank Transformation (Laishevo and Ostolopovo Archaeological Sites, Tatarstan, Russia). In Proceedings of the Earth Resources and Environmental Remote Sensing/GIS Applications XII, Online Only, 12 September 2021; Schulz, K., Nikolakopoulos, K.G., Michel, U., Eds.; SPIE: Madrid, Spain, 2021; p. 57.
54. Panagos, P.; Borrelli, P.; Meusburger, K.; Alewell, C.; Lugato, E.; Montanarella, L. Estimating the Soil Erosion Cover-Management Factor at the European Scale. *Land Use Policy* **2015**, *48*, 38–50. [CrossRef]
55. Litvin, L.F.; Kiryukhina, Z.P.; Krasnov, S.F.; Dobrovol'skaya, N.G. Dynamics of Agricultural Soil Erosion in European Russia. *Eurasian Soil Sci.* **2017**, *50*, 1344–1353. [CrossRef]
56. Panagos, P.; Borrelli, P.; Meusburger, K.; Yu, B.; Klik, A.; Jae Lim, K.; Yang, J.E.; Ni, J.; Miao, C.; Chattopadhyay, N.; et al. Global Rainfall Erosivity Assessment Based on High-Temporal Resolution Rainfall Records. *Sci. Rep.* **2017**, *7*, 4175. [CrossRef]
57. Park, H.; Sherstiukov, A.B.; Fedorov, A.N.; Polyakov, I.V.; Walsh, J.E. An Observation-Based Assessment of the Influences of Air Temperature and Snow Depth on Soil Temperature in Russia. *Environ. Res. Lett.* **2014**, *9*, 064026. [CrossRef]
58. Golosov, V.; Yermolaev, O.; Litvin, L.; Chizhikova, N.; Kiryukhina, Z.; Safina, G. Influence of Climate and Land Use Changes on Recent Trends of Soil Erosion Rates within the Russian Plain. *Land Degrad. Dev.* **2018**, *29*, 2658–2667. [CrossRef]
59. Magritsky, D.V.; Banshchikov, L.S. Response of Sediment Yield in the Lena River Basin to Climate Change and Economic Activity. Dynamics and interaction of geospheres of the Earth. In Proceedings of the All-Russian Conference with International Participation Dedicated to the 100th Anniversary of the Training of Specialists in the Field of Earth Sciences at Tomsk State University, Tomsk, Russia, 8–11 November 2021; pp. 61–65. (In Russian)
60. Chalov, S.; Prokopeva, K.; Habel, M. North to South Variations in the Suspended Sediment Transport Budget within Large Siberian River Deltas Revealed by Remote Sensing Data. *Remote Sens.* **2021**, *13*, 4549. [CrossRef]
61. Larionov, G.A. *Water and Wind Erosion: Main Features and Quantitative Assessment*; MSU Publishing House: Moscow, Russia, 1993; ISBN 978-5-211-02467-0. (In Russian)
62. Nachtergaele, F.; Velthuizen, H.; Verelst, L.; Batjes, N.; Dijkshoorn, K.; Engelen, V.W.P.; Fischer, G.; Jones, A.; Montanarela, L.; Petri, M.; et al. *The Harmonized World Soil Database*; FAO: Rome, Italy; IIASA: Laxenburg, Austria, 2009; p. 37.
63. Warren, S.D.; Ruzycki, T.S.; Vaughan, R.; Nissen, P.E. Validation of the Unit Stream Power Erosion and Deposition (USPED) Model at Yakima Training Center, Washington. *Northwest Sci.* **2019**, *92*, 338–345. [CrossRef]
64. Alatorre, L.C.; Beguería, S.; García-Ruiz, J.M. Regional Scale Modeling of Hillslope Sediment Delivery: A Case Study in the Barasona Reservoir Watershed (Spain) Using WATEM/SEDEM. *J. Hydrol.* **2010**, *391*, 109–123. [CrossRef]